MDPI

Article

Impact of Elastic Diaphragm Hardness and Structural Parameters on the Hydraulic Performance of Automatic Flushing Valve

Hao Gao [1,2], Yan Mo [2,*], Feng Wu [1,*], Jiandong Wang [3] and Shihong Gong [2]

[1] School of Water Conservancy, North China University of Water Resources and Electric Power, Zhengzhou 450046, China
[2] State Key Laboratory of Simulation and Regulation of Water Cycle in River Basin, China Institute of Water Resources and Hydropower Research, Beijing 100048, China
[3] Institute of Environment and Sustainable Development in Agriculture, Chinese Academy of Agricultural Sciences, Beijing 100081, China
* Correspondence: moyansdi@163.com (Y.M.); wufeng@ncwu.edu.cn (F.W.)

Abstract: Automatic flushing valve (AFV) can improve the anti-clogging ability of the drip fertigation system. The minimum inlet pressure (H_{amin}) required for automatic closing and the maximum flushing duration (FD_{max}) are two important performance indexes of AFV. The existing AFV products have the problem of larger H_{amin} and smaller FD_{max}, which result higher investment and operating cost, and poor flushing efficiency. Based on the mechanical analysis of the AFV elastic diaphragm and the derivation of the FD, elastic diaphragm hardness (E), ascending channel offset distance (D), and drain hole width (W) were selected as the experimental factors, and nine AFVs were designed by $L_9(3^3)$ orthogonal test method to investigate the influence of elastic diaphragm hardness and structural parameters on the hydraulic performance of AFVs. The hydraulic performance test results showed that the H_{amin} of the nine AFVs ranged from 0.026 to 0.082 MPa and FD_{max} ranged from 36.3 to 95.7 s. H_{amin} was positively correlated with E and D and negatively correlated with W. FD_{max} was negatively correlated with E and W and tended to increase and then decrease with D. All elastic diaphragm hardness and structural parameters had a significant effect on H_{amin}, and E and W had a significant effect on FD_{max}. Based on the range analysis, two new combinations of AFV elastic diaphragm hardness and structural parameters with minimum H_{amin} (E = 40 HA, D = 0 mm, W = 2 mm) and maximum FD_{max} (E = 40 HA, D = 2 mm, W = 1.68 mm) were determined, and the corresponding H_{amin} was 0.022 MPa, 63.3% lower than that of the existing product, and FD_{max} was 116.4 s, 71.2% higher than that of the existing product. In this study, two ternary nonlinear mathematical regression models of H_{amin} and FD_{max} with elastic diaphragm hardness and structural parameters was constructed. The simulation accuracy of the models is good and can be used to quickly predict the optimal combination of AFV parameters to satisfy the actual engineering-required H_{amin} and FD_{max}.

Keywords: drip irrigation; drip fertigation system; clogging; minimum closing pressure; maximum flushing duration

1. Introduction

Drip fertilization can improve the uniformity of water and fertilizer distribution in crop root zone [1], improve the current status of water and fertilizer resources utilization in dryland agriculture, and promote the improvement of crop yield and quality. In recent years, drip fertilization has developed rapidly in China [2–4]. By the end of 2020, the application area of fertigation technology in China exceeded 10 million ha. When fertilizer enters the dripline with irrigation water, the precipitation process of suspended particles of sediment and other suspended impurities in the water is susceptible to fertilizer in the

pipe network, the mechanism of emitter clogging is more complex, and the probability of clogging may be higher [5]. Ca^{2+}, Mg^{2+}, K^+ and SO_4^{2-} in fertilizers form large sediment particle agglomerates with sulfate and other precipitates, which accelerate the formation of clogging silt in the flow channel [5–8], which in turn reduces the turbulence of water flow and makes sediment particles prone to siltation in the dripline and flow channels [9,10].

Regular acid-chlorine treatment is one of the most commonly used blockage control methods for drip fertigation systems [11–13]. Magnetized water can inhibit the formation of scale [14], and a suitable intensity of magnetization can improve the anti-clogging performance of drip fertigation systems [15]. In addition, techniques such as micro- and nanobubble sterilization and electrochemical removal have also been used to purify water and remove clogging substances attached to the inner wall surface of the dripline [16,17]. These anti-clogging methods for drip fertigation systems are mainly controlled by inhibiting the production of clogging materials, promoting the decomposition of existing clogging materials, or promoting the separation of precipitates from the pipe wall.

Dripline flushing technology, which accelerates the speed of water flow in the pipe network to improve the hydraulic shear force and strip sediment on the pipe wall while providing a discharge path for clogging suspended matter and further reducing the chances of clogging material into the emitter flow channel, is a simple, convenient and effective method for emitter anti-clogging performance [17–20]. At present, most of the flushing operations adopt the method of manually opening and closing the end of the driplines [21]. However, most projects can only be flushed once at the beginning or end of the irrigation season due to its cumbersome flushing operation and large consumption of manpower and material resources. It often fails to achieve the desired flushing effect [22]. The automatic flushing valve (AFV) is installed at the end of one or more driplines to automatically open and flush the pipes when the drip irrigation system is activated, and then automatically close after the designed length of time (FD) [23,24]. When the inlet pressure (H_a) is 0.06–0.1 MPa, the FD of both AFVs produced by Naandanjain (NaanDanJain Irrigation, Ltd., Post Naan, Israel) and Netafim (Netafim Ltd., Tel Aviv, Israel) is less than 10 s, which is much less than the FD requirement of 3–6 min proposed by scholars [11,13,25–28]. Zhao developed an AFV with a FD of 53 s by improving the delay channel structure [29], Mo et al. increased the water storage volume by adding an exhaust device to the upper cavity of the AFV, and the FD could be increased to 68 s [24]. After 400 h of continuous operation with a water source of 1 kg/m^3 sand content, the average relative flow rate of the emitter on a 12 m long dripline with an AFV was 16.6% higher than that without an AFV [29]; the average relative flow rate of the emitter on a 48 m long dripline with an AFV was increased by 4.0% compared to that without an AFV [30]. The installation of an AFV can substantially improve the dripline blockage resistance, but the effect decreases with increasing dripline length. The FD of the existing AFV may still be short for the common dripline length of 60~80 m in actual projects, which cannot meet the flushing demand. In addition, there has been a lack of in-depth research on the intrinsic mechanisms to improve the FD by optimizing the AFV elastic diaphragm hardness and structural parameters.

As the AFV needs to rely on the gradual accumulation of water pressure in the upper cavity to push the elastic diaphragm downwards expansion movement to achieve the delayed automatic closing function, the minimum value of the inlet pressure required for automatic closing is H_{amin}. When the drip irrigation system is equipped with AFVs, the water supply pressure of the pump not only needs to meet the design pressure value (e.g., 0.1 MPa) of the emitter farthest from the pump but also the H_{amin} of the AFV farthest from the pump. In addition, the increased water velocity in the pipeline during flushing can substantially increase the head loss along the pipeline network, which in turn increases the pump water supply pressure demand. Then, reducing H_{amin} can reduce the pump input cost and operation cost of an automatic flushing drip irrigation system and promote the application of automatic flushing technology, but no research related to H_{amin} of the AFV has been reported.

Based on this, the mechanical parameters of elastic diaphragm and structural parameters affecting the hydraulic performance of the AFV were screened through force analysis of the elastic diaphragm, and different AFVs composed of different elastic diaphragm hardness (E), ascending channel offset distance (D) and width of drain hole (W) were set up with the help of orthogonal tests, and the tests were processed. The effects of elastic diaphragm hardness and structural parameters on H_{amin} and FD_{max} were studied, and the mechanism of structural parameter optimization on the hydraulic performance of AFV was investigated. The mathematical model of quantitative characterization of H_{amin} and FD_{max} with the change of elastic diaphragm hardness and structural parameters was constructed. This provides a theoretical basis for AFV update iteration and technical support for alleviating the problem of drip irrigation water and fertilizer integration clogging.

2. Materials and Methods

2.1. The Working Principle of the Automatic Flushing Valve

Automatic flushing valve (AFV) is mainly consisting of valve body, elastic diaphragm, valve cover and threaded ring. The raised edge of the elastic diaphragm is fixed between the valve body and the valve cover by the threaded ring. When the pump starts, the AFV starts flushing, and the water flow from the end of the dripline enters the AFV inlet and then divides into two paths of movement (as shown by the blue arrow in Figure 1a): firstly, a small portion of the water flow enters the delay channel through the ascending channel and moves counterclockwise for one turn before entering the upper cavity; secondly, a large amount of water flow carries the suspended clogging matter from the pipes and is discharged from the drain hole through the outlet.

(**a**) Front section view before AFV starts to flush   (**b**) Side section view before AFV starts to flush

(**c**) Initial volume of the upper cavity   (**d**) Water storage volume of the AFV body
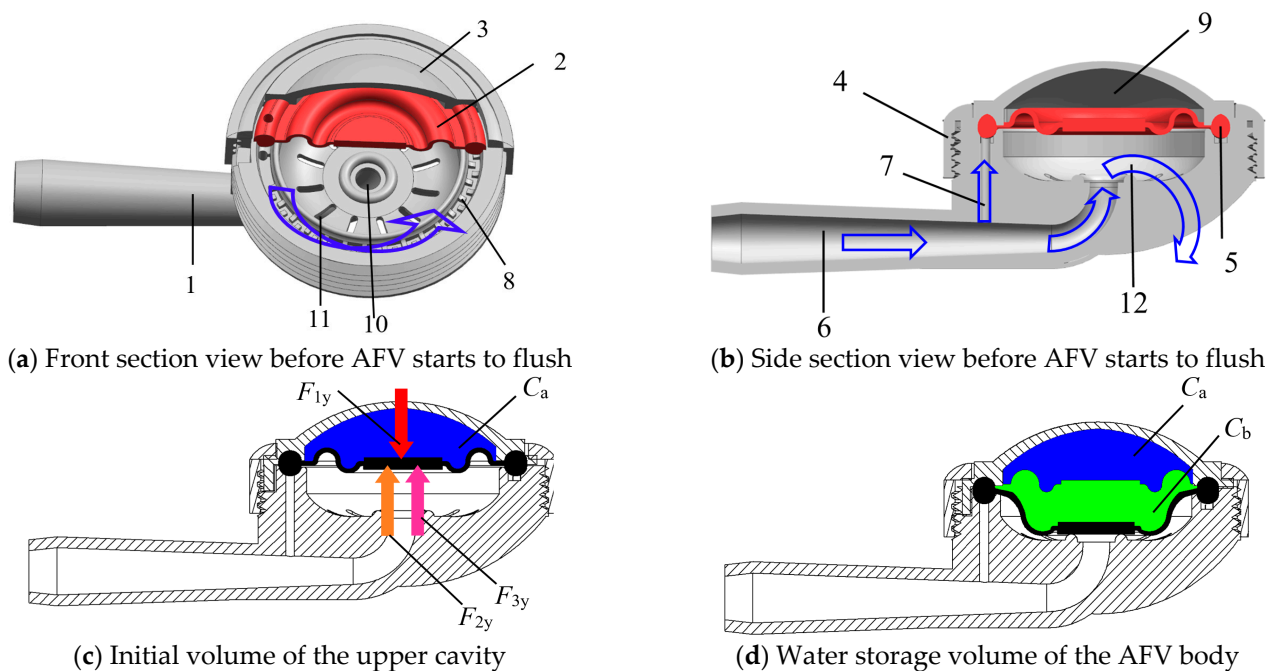
Figure 1. Schematic diagram of the automatic flushing valve (AFV) structure. 1. Valve body; 2. Elastic diaphragm; 3. Valve cover; 4. Threaded ring; 5. Raised edge of the elastic diaphragm; 6. Water inlet; 7. Ascending channel; 8. Delay channel; 9. Upper cavity; 10. Outlet; 11. Drain hole; and 12. Lower cavity. Note: C_a is the initial volume of the upper cavity, mL; C_b is the volume added by the downwards movement of the elastic diaphragm, mL; F_{1y} is the downwards vertical force exerted by water in the upper cavity on the elastic diaphragm, N; F_{2y} is the vertical upwards force of water in the lower cavity on the elastic diaphragm, N; F_{3y} is the vertical elastic force of the elastic diaphragm, N; and the blue arrow is the direction of water movement.

As the amount of water in the upper cavity gradually increases, the elastic diaphragm gradually moves downwards under the resultant force in the vertical direction (F_y) (Equation (4)). F_y is composed of the upper cavity water pressure ($F1y$) (Equation (1)), the lower cavity water pressure ($F2y$) (Equation (2)), and the elastic force of the elastic diaphragm ($F3y$) (Equation (3)). Since the F_y is greater than zero, the H_a (inlet pressure at the beginning of flushing for the AFV to automatically close) can be calculated in Equation (5).

$$F_{1y} = (H_a - h_{f1} - h_{f2}) \times S_x \tag{1}$$

$$F_{2y} = \left(H_a - h_{f1}\right) \times (S_x - S_{drainx}) \tag{2}$$

$$F_{3y} = a \times E + b \tag{3}$$

$$F_y = F_{1y} - F_{2y} - F_{3y} > 0 \tag{4}$$

$$Ha > hf1 + \frac{hf2 \times Sx + a \times E}{S_{drainx}} \tag{5}$$

where F_{1y} is the downwards vertical force (N) exerted by water in the upper cavity on the elastic diaphragm. F_{2y} is the vertical upwards force of water in the lower cavity on the elastic diaphragm (N). F_{3y} is the vertical elastic force of the elastic diaphragm (N); E is the hardness of the elastic diaphragm (HA); F_y is the vertical downwards resultant force of the elastic diaphragm (N); a and b are the primary term coefficient and constant term, respectively, $a > 0$ [31]; H_a is the AFV inlet pressure (MPa); h_{f1} is the water loss generated in the water inlet (MPa) in Figure 1b; h_{f2} is the water loss generated in the ascending channel in Figure 1b and delay channel (MPa) in Figure 1a; S_x is the projection area of the elastic diaphragm on the horizontal plane (m^2); and $S_{drain x}$ is the projection area of the drain hole on the horizontal plane (m^2).

The time used from the beginning to the end of the AFV is the flushing duration (FD, s), which is the quotient of the water storage volume (C_w, mL) and the average flow rate of water entering the upper cavity from the end of the delay channel (q, mL/s) (Equation (6)). According to the result from Mo et al. [24], C_w is approximately equal to the volume added by the downwards movement of the elastic diaphragm (C_b, mL) based on the initial volume of the upper cavity (C_a, mL).

$$FD = C_w/q \approx C_b/q \tag{6}$$

2.2. Analysis of Parameters Affecting the Hydraulic Performance of AFVs

H_a and FD are the key design parameters for automatic flushing drip irrigation system (AFDS). From Equation (5), it can be seen that H_a increases with the decrease in S_{drainx} and the increase in E. Furthermore, this can be achieved by setting different drain hole widths (W) and elastic diaphragm materials. From Equation (6), FD can increase with the increase in C_b and decrease in q. When H_a is the same, C_b may be influenced by E. In addition, this paper intends to increase h_{f2} by setting a different ascending channel offset distance (D) to reduce the delay channel inlet pressure and thus reduce q.

2.2.1. Experimental Design

Referring to the research results of Zhao et al. and Mo et al. [23,24], E is set to a total of three levels, 40, 55, and 60 HA, D is set to a total of three levels, 0, 2, and 4 mm (Figure 2a–c), and W is set to a total of three levels, 1, 1.68, and 2 mm (Figure 2d–f). The experiment is designed using orthogonal experimental Table L9 (3^3), and the experimental design is shown in Table 1. The elastic diaphragm hardness test is carried out using a Shore durometer on the "A" scale. The range of Shore durometer (Yueqing Handpi Instrument Co., Ltd., Zhejiang, China) is 0–100 HA with an accuracy of 0.5 grade.
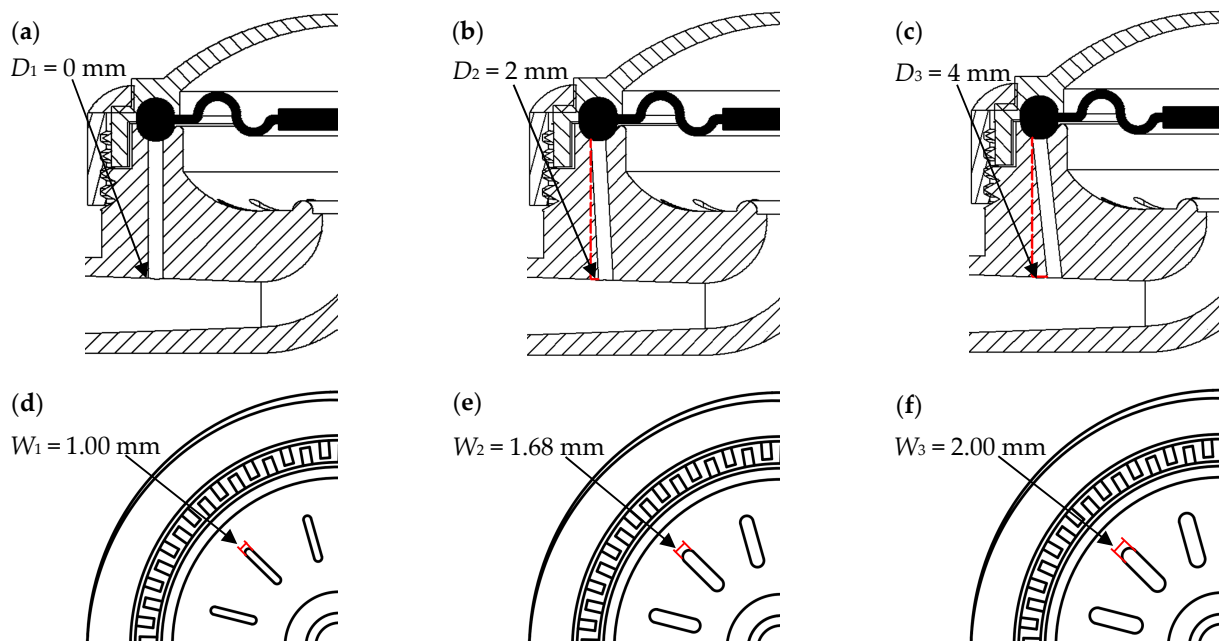
Figure 2. Schematic diagram of the variation in different ascending channel offset distances (D) (D_1, D_2 and D_3) and different drain hole widths (W) (W_1, W_2 and W_3) of the AFV.

Table 1. Experimental design.

Order	Treatments	Experimental Factors		
		E (HA)	D (mm)	W (mm)
1	$E_1D_1W_1$	40	0	1.00
2	$E_1D_2W_2$	40	2	1.68
3	$E_1D_3W_3$	40	4	2.00
4	$E_2D_1W_3$	55	0	2.00
5	$E_2D_2W_1$	55	2	1.00
6	$E_2D_3W_2$	55	4	1.68
7	$E_3D_1W_2$	60	0	1.68
8	$E_3D_2W_3$	60	2	2.00
9	$E_3D_3W_1$	60	4	1.00

2.2.2. Experimental Method and Measurement Index

The AFV hydraulic performance experiment was conducted at the China National Water Conservation Irrigation Engineering Research Center (Beijing, China) with a local tap water source, and the water temperature was maintained at (23 ± 2) °C [32,33]. The 3D model of the AFV used for the experiment was designed with UG NX 10.0 software (Siemens PLM Software, Germany) and processed with 3D printing technology (accuracy of 0.1 mm) using DSM IMAGE8000 photosensitive resin (Royal DSM Group, Netherlands). Before experiment, three AFVs with the same specifications were installed at the end of the PE pipe (Figure 3), the ball valve was closed, and the three buckets were placed directly under each of the three AFVs. The centrifugal pump (CDLF4 10, South Pump Industry Co., Ltd., Zhejiang, China) was started, and the pressure gauge was set (range 0~0.25 MPa, accuracy 0.4 grade, Yangquan Instrument Co., Ltd., Shanxi, China) through the valve to read H. At the same time, the three ball valves were quickly opened, the AFVs began to work, and the timer started. At this time, the pressure gauge readings from H quickly decreased to H_a, and the AFVs discharged water into the bucket. When the AFV was closed and no water flowed out, the timing stopped, the timer time was the FD. At this point, the pressure gauge reading returned to H. Each experiment was repeated three times. During the experiment, the minimum H_a to control the AFV automatic closure was H_{amin}, and the corresponding flushing duration was FD_{max}.
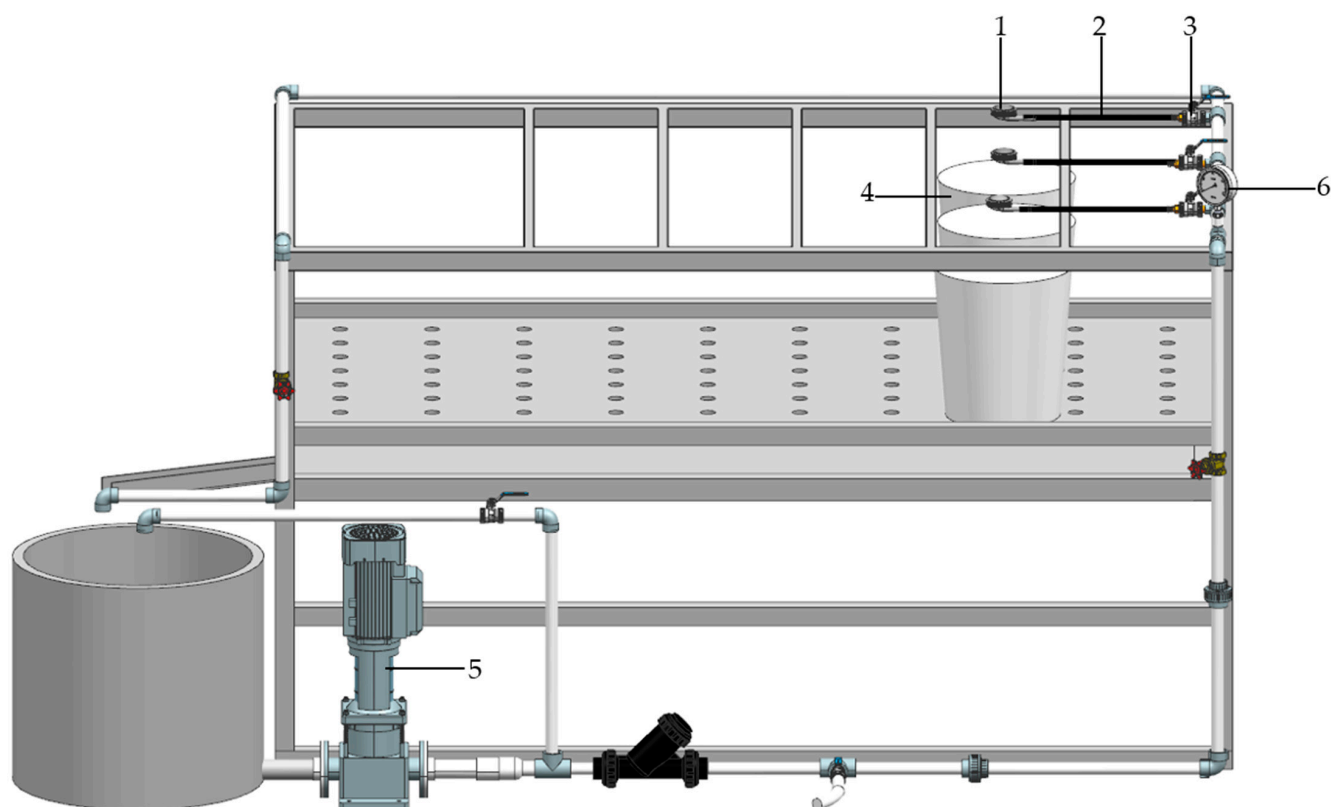
Figure 3. Schematic diagram of the hydraulic experimental platform of the AFV. 1. Automatic flushing valve; 2. PE pipe; 3. ball valve; 4. bucket; 5. centrifugal pump; and 6. pressure gauge.

2.3. Data Analysis

All statistical analyses and the function describing the relationship of hydraulic performance with the mechanical parameters of elastic diaphragm and structural parameters were performed by SPSS 26.0 statistical software (SPSS, Inc., Chicago, IL, USA). The construction of mathematical models was also completed by SPSS 26.0 statistical software. The consistency between the experimental results and the prediction results of the mathematical model was evaluated by the root mean square error (RMSE) and the normalized root mean square error (nRMSE). (Equations (7) and (8)) [34–36].

$$\text{RMSE} = \sqrt{\frac{\sum\limits_{i=1}^{n}(S_i - E_i)^2}{n}} \tag{7}$$

$$\text{nRMSE} = \frac{\sqrt{\frac{\sum\limits_{i=1}^{n}(S_i - E_i)^2}{n}}}{E_{\text{ave}}} \times 100\% \tag{8}$$

where S_i and E_i were the simulated and measured values, respectively; i was the number of the measured value, n was the total number of measured values; and E_{ave} was the average of all measured values. The model evaluation criteria were as follows: nRMSE $\leq$ 10%, excellent agreement between the simulated and measured rates; 10% < nRMSE < 20%, good; 20% $\leq$ nRMSE $\leq$ 30%, fair; and nRMSE > 30%, poor.

3. Results and Analysis

3.1. Hydraulic Performance Experimental Results

The range of H_{amin} and FD_{max} for nine AFVs is 0.026~0.082 MPa and 36.3~95.7 s (Table 2), respectively. Figure 4 shows that FD_{max} and H_{amin} are negatively correlated; $E_1D_1W_1$ has the smallest H_{amin}, 0.026 MPa, and the largest FD_{max}, 95.7 s.

Table 2. Hydraulic performance experimental results for the AFVs.

Treatments	H_{amin} (MPa)	FD_{max} (s)
$E_1D_1W_1$	0.026	95.7
$E_1D_2W_2$	0.031	83.3
$E_1D_3W_3$	0.041	87.3
$E_2D_1W_3$	0.033	38.7
$E_2D_2W_1$	0.040	82.7
$E_2D_3W_2$	0.065	58.7
$E_3D_1W_2$	0.040	54.3
$E_3D_2W_3$	0.048	48.7
$E_3D_3W_1$	0.082	36.3

(**a**) H_{amin} (**b**) FD_{max}
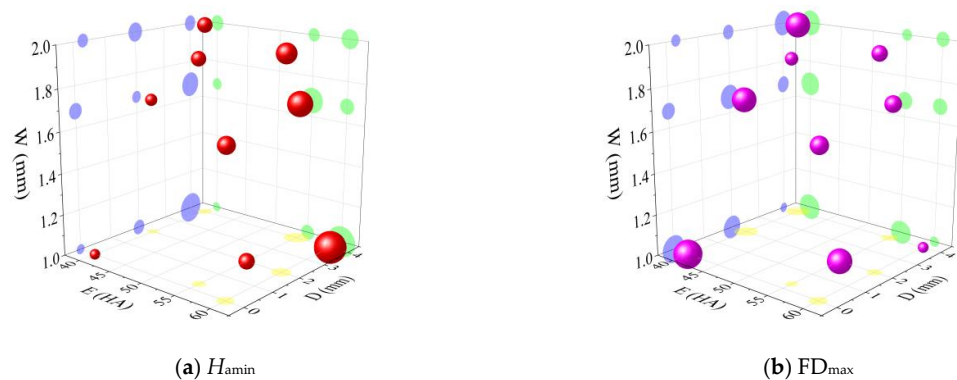
Figure 4. Automatic flushing valve minimum closing pressure (H_{amin}) (**a**) and maximum flushing duration (FD_{max}) (**b**), three-dimensional distribution of experimental results. Note: The diameter of the sphere or circle is proportional to the value of H_{amin} (**a**) or FD_{max} (**b**); the red sphere represents H_{amin}; the magenta sphere represents FD_{max}; the blue, yellow and green circles represent the projections of H_{amin} (**a**) or FD_{max} (**b**) on the three faces of *D-W*, *E-D* and *E-W*, respectively.

3.2. Analysis of the Hydraulic Performance Range of AFVs

Through range analysis, we can obtain the influence of the change in the level of the experimental factor on the index to determine the optimal level of the factor and obtain the primary and secondary order of the factors affecting the hydraulic performance of the AFV. As shown in Table 3, H_{amin1}, H_{amin2}, and H_{amin3} and FD_{max1}, FD_{max2}, and FD_{max3} are the average values of H_{amin} and FD_{max}, respectively, when each experimental factor is taken at the 1, 2 and 3 levels, such that $H_{amin1} = (0.026 + 0.031 + 0.041)/3 = 0.033$ MPa, where 0.026, 0.031 and 0.041 MPa are the H_{amin} values at $E = 40$ HA (Table 2), respectively. R is the range of the corresponding factor; a larger R indicates that the experimental factor in the design range of the change leads to greater changes in the value of the experimental index and a greater degree of influence of the factor on the hydraulic performance of the AFV. The range analysis results show that the main order of the effect of each experimental factor on H_{amin} and FD_{max} is D, E, and W, and E, W, and D, respectively.

Table 3. Minimum closing pressure (H_{amin}) and maximum flushing duration (FD_{max}) range analysis of the automatic flushing valve.

Experimental Indexes		Experimental Factors		
		E (HA)	*D* (mm)	*W* (mm)
H_{amin}	H_{amin1}	0.033	0.033	0.049
	H_{amin2}	0.046	0.040	0.045
	H_{amin3}	0.057	0.063	0.041
	R	0.024	0.030	0.008
FD_{max}	FD_{max1}	88.8	62.9	71.6
	FD_{max2}	60.0	71.6	65.4
	FD_{max3}	46.4	60.8	58.2
	R	42.4	10.8	13.4

Note: Subscripts 1~3 are 3 levels, same below.

The trend diagram of factors and experimental indexes with the experimental factors as horizontal coordinates and the experimental indexes as vertical coordinates is shown in Figure 5. H_{amin} is positively correlated with *E* and *D* and negatively correlated with *W*. FD_{max} is negatively correlated with *E* and *W* and shows a trend of increasing and then decreasing with *D*. When *E* is reduced from 60 HA to 40 HA, the reduction of H_{amin} is 42.1% and the increase of FD_{max} is 91.4%; when *D* is reduced from 4 mm to 0 mm, the reduction of H_{amin} is 47.6% and the increase of FD_{max} is 3.5%; and when *W* is increased from 1 mm to 2 mm, the reduction of H_{amin} is 16.3%, at which time FD_{max} decreases by 18.7%.
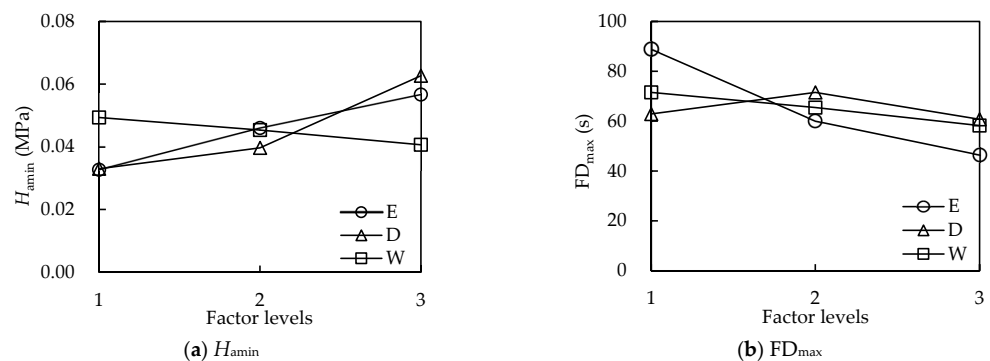
(**a**) H_{amin}

(**b**) FD_{max}

Figure 5. Effect of different factor levels on the minimum closing pressure (H_{amin}) (**a**) and maximum flushing duration (FD_{max}) (**b**) of the automatic flushing valve (AFV).

The optimal factor combination is $E_1D_1W_3$ when the smaller H_{amin} is the optimal principle and $E_1D_2W_1$ when the larger FD_{max} is the optimal principle, and these two AFVs are not in Table 2.

3.3. Variance Analysis of the Hydraulic Performance of the Automatic Flushing Valve

To further explore whether the influence of experimental factors on hydraulic performance is statistically significant, this study conducts variance analysis at significance levels of 0.05 and 0.1. As shown in Table 4, *E*, *D* and *W* have significant effects on H_{amin}. *E* and *W* have a significant effect on FD_{max}, while *D* has no significant effect on FD_{max}.

Table 4. Variance analysis of the influence of experimental factors on minimum closing pressure (H_{amin}) and maximum flushing duration (FD_{max}).

Experimental Indexes	*E*	*D*	*W*
H_{amin}	78.236 **	131.082 **	10.180 **
FD_{max}	33.773 **	2.357	3.219 *

Note: * and ** represent $p < 0.1$ and $p < 0.05$, respectively.

3.4. Construction and Verification of a Mathematical Regression Model for Hydraulic Performance of AFV

The suitable flushing duration per unit length of dripline ($T = FD/m$, where m is the number of driplines controlled by one AFV; FD is the time taken from the beginning to the end of flushing by the AFV (s); and T is the flushing duration per unit length of dripline (s/m).) is determined by the water quality conditions, fertilizer type, water and fertilizer system, blockage formation characteristics and other factors together. The pump water supply pressure in AFDS is influenced by the size and parameters of the pipe network system, H_{amin}, m, etc. The smaller H_{amin} is, the less pressure is required for the pump of the drip irrigation system, and the lower the system investment and freight cost. When the T is certain, the m increases with increasing FD; thus, the number of AFVs required for the system decreases, and the investment is reduced. Therefore, it is necessary to determine the appropriate H_{amin} and FD_{max} according to the actual project requirements and then determine the AFV elastic diaphragm hardness and structural parameters. In this study, the multivariate nonlinear regression models of H_{amin} and FD_{max} with E, D, and W are constructed with the help of SPSS 26.0 statistical software, and the coefficients of determination (R^2) of H_{amin} and FD_{max} regression models are 0.953 and 0.829, respectively, which means well fitted.

Within the range of factors and level parameters in Table 1, this paper additionally processes 15 different specifications of AFVs for hydraulic performance experimentation, and the measured results and the predicted results from Equations (9) and (10) are shown in Table 5 and Figure 6. The relative errors between the measured and predicted values of H_{amin} and FD_{max} are −12.2% to 19.0% and −18.4% to 18.3%, respectively, with a small root mean square error (RMSE) of 0.003 MPa and 10.2 s, respectively, and the normalized root mean square error (nRMSE) is 8.0% and 14.5%, respectively, both less than 20%. The range analysis results show that the combination with the smallest H_{amin} result is $E_1D_1W_3$ and the combination with the largest FD_{max} is $E_1D_2W_1$. As shown in Table 5, the measured H_{amin} of $E_1D_1W_3$ is 0.022 MPa, and the measured FD_{max} of $E_1D_2W_1$ is 116.4 s, which are lower and larger than the values in Table 2, respectively. The regression Equations (9) and (10) can be used to predict the combination of AFV elastic diaphragm hardness and structural parameters corresponding to H_{amin} and FD_{max} required for the actual project and can shorten the development time.

$$H_{amin} = 0.002D^2 - 0.009 \times W^2 + 0.001 \times E + 0.005 \times D + 0.025 \times W + 0.004 \times E \times D \times W - 0.031 \tag{9}$$

$$FD_{max} = -0.037 \times E^2 - 2.244 \times D^2 - 11.625 \times W^2 + 1.493 \times E - 0.389 \times D + 13.556 \times W + 0.114 \times E \times D \times W + 95.205 \tag{10}$$

Table 5. Model Validation.

Treatments	E (HA)	D (mm)	W (mm)	H_{amin} Predicted Value (MPa)	H_{amin} Measured Value (MPa)	H_{amin} Relative Error (%)	FD_{max} Predicted Value (s)	FD_{max} Measured Value (s)	FD_{max} Relative Error (%)
$E_1D_1W_2$	40	0	1.68	0.024	0.026	−9.3	86.4	73.0	18.3
$E_1D_1W_3$	40	0	2.00	0.021	0.022	−2.7	77.0	94.3	−18.4
$E_1D_2W_1$	40	2	1.00	0.033	0.028	19.0	97.7	116.4	−16.1
$E_1D_3W_2$	40	4	1.68	0.051	0.047	9.3	79.6	90.3	−11.9
$E_2D_1W_1$	55	0	1.00	0.036	0.036	−0.4	68.6	80.4	−14.6
$E_2D_1W_2$	55	0	1.68	0.037	0.036	3.3	56.6	58.7	−3.5
$E_2D_2W_2$	55	2	1.68	0.043	0.040	7.3	68.0	73.3	−7.3
$E_2D_2W_3$	55	2	2.00	0.038	0.039	−1.9	62.6	55.3	13.3
$E_2D_3W_3$	55	4	2.00	0.058	0.053	9.1	60.0	65.5	−8.4
$E_3D_1W_1$	60	0	1.00	0.040	0.046	−12.2	55.0	62.7	−12.2
$E_3D_1W_3$	60	0	2.00	0.040	0.039	1.4	33.7	33.9	−0.4
$E_3D_2W_1$	60	2	1.00	0.051	0.047	9.5	59.0	67.8	−13.1
$E_3D_2W_2$	60	2	1.68	0.047	0.044	7.8	56.3	67.6	−16.7
$E_3D_3W_2$	60	4	1.68	0.070	0.065	6.9	51.6	58.0	−11.0
$E_3D_3W_3$	60	4	2.00	0.062	0.061	2.2	51.0	57.8	−11.8
RMSE				0.003 MPa			10.2 s		
nRMSE (%)				8.0			14.5		
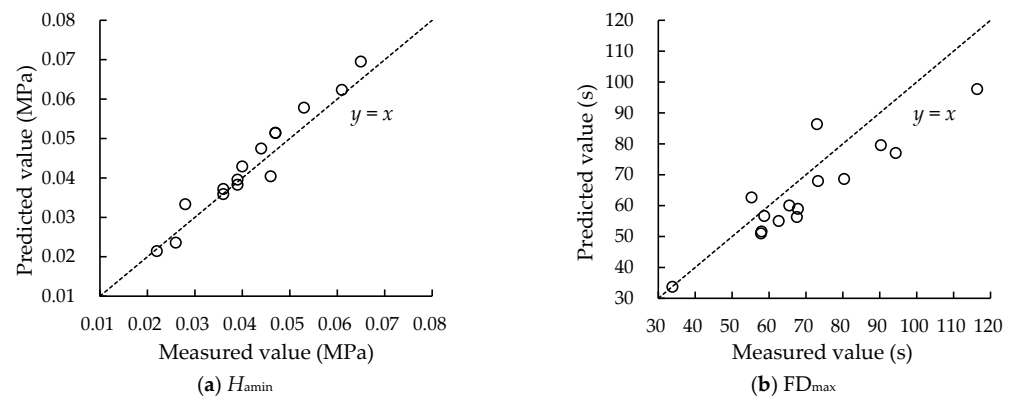
Figure 6. Comparison of measured and predicted values by the regression model for the automatic flushing valve.

4. Discussion

Both Zhao et al. and Mo et al. focused on the increase in FD_{max} for the AFV without considering the decrease in H_{amin} [23,24]. Compared with the conventional drip irrigation system without AFVs, the AFV in the flushing process, the water flow in the pipe network system increases significantly, resulting in a significant increase in the head loss (h_f) between the pump and the AFVs inlet. To meet the H_{amin} of the farthest AFV from the pump, the pump water supply pressure of AFDS (H) should be greater than ($H_{amin} + h_f$). It is necessary to reduce the H_{amin} and then reduce the pump input and operating costs.

From the mechanical analysis of the AFV elastic diaphragm and the experiment results, it can be seen that H_{amin} decreases with the decrease in h_{f1}, h_{f2}, S_x and E and decreases with the increase in S_{drainx}. When E decreases from 60 HA to 40 HA, H_{amin} decreases by 42.1% on average; D decreases from 4 mm to 0 mm leading to the decrease of h_{f2}, and thus H_{amin} decreases by 47.6% on average; W increases from 1 mm to 2 mm leading to an increase in S_{drainx} and an average decrease in H_{amin} of 16.3%; and the effects of H_{amin} by E, D and W all reach significance levels.

Increasing T promotes the discharge of fine-grained sediments from drip irrigation pipes [27], and in addition, increasing FD increases m when T is certain (see Section 3.4), which in turn reduces the number of AFVs and reduces the investment in AFDS. Assuming that the air in the upper cavity of the AFV cannot be discharged and that the compression factor of air is close to 1, the FD is mainly influenced by C_b and q (Equation (7)). When H_a is the same, the AFV flushing is over, and the elastic diaphragm is in close contact with the outlet and the expansion of the elastic diaphragm on the horizontal plane increases as E decreases, which in turn increases C_b (Figure 1d); therefore, when E decreases from 60 HA to 40 HA, FD_{max} increases significantly by 91.2% on average. When W decreases from 2 mm to 1 mm, FD_{max} increases by 22.9% on average, probably because the elastic diaphragm moves downwards under the action of F_y (Figure 1c,d), and F_y decreases with the increase of F_{2y} (Equation (4)); therefore, when the AFV is guaranteed to close automatically, increasing F_{2y} within a certain range can slow down the process of downwards movement of the elastic diaphragm and increase the FD. F_{2y} increases as W decreases (Equation (2)), F_{2y} increases as the force F_y on the elastic diaphragm decreases, and the AFV automatically closes the longer the flushing duration is needed; therefore, FD_{max} increases as W decreases. h_{f2} increases as D increases. When H_a is the same, q decreases as D increases, resulting in FD increases as D increases. When D increases from 1 mm to 2 mm, FD_{max} increases by 13.8%; however, when D increases from 2 mm to 4 mm, h_{f2} increases, and H_{amin} increases from 0.040 MPa to 0.063 MPa before the AFV can close automatically (Table 3), and the increase in q causes the FD to decrease.

In this study, two combinations of AFV elastic diaphragm hardness and structural parameters are obtained in the extreme difference analysis with the objectives of H_{amin} and FD_{max}: $E_1D_1W_3$ and $E_1D_2W_1$, respectively. The measured H_{amin} of the $E_1D_1W_3$ AFV

is 0.022 MPa, which is 15.4% lower than the lowest value of H_{amin} in Table 2 and 63.3% lower than the existing AFV [29]. The measured FD_{max} of $E_1D_2W_1$ is 116.4 s, which is 21.6% higher than the maximum value of FD_{max} in Table 2 and 71.2% higher than the existing AFV [24].

In actual projects, the appropriate H_{amin} needs to be determined according to the scale of the pipe network system and parameters such as length and diameter of pipes at all levels, and the appropriate FD_{max} needs to be determined by considering the system investment and operation cost. The appropriate FD_{max} also needs to be determined by considering the water quality conditions of water sources, fertilizer types, clog formation characteristics, system investment, and other factors through a large number of experiments [13,25,26,28]. The quantitative regression model of H_{amin}, FD_{max} and AFV elastic diaphragm hardness and structural parameters constructed in this study has a good prediction accuracy [34–36], which can help manufacturers to produce AFVs for practical engineering needs at low cost and quickly by providing a theoretical basis and prediction guidance. In future research, it is necessary to construct a hydraulic calculation model of AFDS to study the dynamic balance relationship of water supply pressure and flow rate required by pumps and H_{amin} under different engineering conditions.

5. Conclusions

Using orthogonal experimental design and hydraulic performance experimental methods, the influencing rule and optimization mechanisms of elastic diaphragm hardness and structural parameters of *E*, *D* and *W* on H_{amin} and FD_{max} were examined, and the main conclusions were drawn as follows:

1. The physical relationship model between H_{amin} and FD_{max} and the elastic diaphragm hardness and structural parameters and the measured results of hydraulic performance show that H_{amin} increases with increasing *E* and *D* and decreases with increasing *W*, FD_{max} decreases with increasing *E* and *W*, and *E*, *D* and *W* have a significant effect on H_{amin}. *E* and *W* have significant effects on FD_{max} ($p < 0.05$);
2. Based on range analysis, the minimum H_{amin} is 0.022 MPa, which is lower than the H_{amin} of the existing AFV by 63.3%. And the maximum FD_{max} is 116.4 s, which is higher than that of the existing AFV by 71.2%.
3. The ternary nonlinear regression equation of hydraulic performance and elastic diaphragm hardness and structural parameters of the AFV has a good prediction accuracy, which can quickly give the structural parameter combination of the AFV required by the actual project and shorten the research and development time.

Author Contributions: Conceptualization, Y.M.; methodology, H.G. and Y.M.; software, H.G.; validation, Y.M., F.W. and S.G.; formal analysis, H.G., Y.M. and J.W.; investigation, H.G. and Y.M.; writing—original draft preparation, H.G.; writing—review and editing, Y.M. and F.W.; funding acquisition, Y.M. All authors have read and agreed to the published version of the manuscript.

Institutional Review Board Statement: Not applicable.

Informed Consent Statement: Not applicable.

Data Availability Statement: The data presented in this study are available upon request from the corresponding author.

Conflicts of Interest: The authors declare no conflict of interest.

Nomenclature

AFV	Automatic flushing valve
H_a	The inlet pressure, (MPa)
H_{amin}	The minimum inlet pressure, (MPa)
FD	The flushing duration, (s)
FD_{max}	The maximum flushing duration, (s)
E	Elastic diaphragm hardness, (HA)
D	Ascending channel offset distance, (mm)
W	Drain hole width, (mm)
AFDS	Automatic flushing drip irrigation system
F_{1y}	The downwards vertical force exerted by water in the upper cavity on the elastic diaphragm, (N)
F_{2y}	The vertical upwards force of water in the lower cavity on the elastic diaphragm, (N)
F_{3y}	The vertical elastic force of the elastic diaphragm, (N)
F_y	The vertical downwards resultant force of the elastic diaphragm, (N)
h_{f_1}	The water loss generated in the water inlet, (MPa)
h_{f_2}	The water loss generated in the ascending channel and delay channel, (MPa)
S_x	The projection area of the elastic diaphragm on the horizontal plane, (m^2)
$S_{drain\ x}$	The projection area of the drain hole on the horizontal plane, (m^2)
C_w	The water storage volume of the AFV body, (mL)
C_a	The initial volume of the upper cavity, (mL)
C_b	The volume added by the downwards movement of the elastic diaphragm, (mL)
C_{air}	The volume of air in the upper cavity, (mL)
q	The average flow rate of water entering the upper cavity from the end of the delay channel, (mL/s)
m	The number of driplines controlled by one AFV
T	The flushing duration per unit length of dripline, (s/m)
H	The pump water supply pressure of AFDS, (MPa)
RMSE	Root mean square error
nRMSE	The normalized root mean square error
h_f	The head loss between the pump and the AFVs inlet, (MPa)

References

1. Fan, J.L.; Wu, L.F.; Zhang, F.C.; Yan, S.C.; Xiang, Y.Z. Evaluation of drip fertigation uniformity affected by injector type, pressure difference and lateral layout. *Irrig. Drain.* **2017**, *66*, 520–529. [CrossRef]
2. Kiboi, M.N.; Ngetich, K.F.; Fliessbach, A.; Muriuki, A.; Mugendi, D.N. Soil fertility inputs and tillage influence on maize crop performance and soil water content in the central highlands of Kenya. *Agric. Water Manag.* **2019**, *217*, 316–331. [CrossRef]
3. Sun, G.Z.; Hu, T.T.; Liu, X.G.; Peng, Y.L.; Leng, X.X.; Li, Y.L.; Yang, Q.L. Optimizing irrigation and fertilization at various growth stages to improve mango yield, fruit quality and water-fertilizer use efficiency in xerothermic regions. *Agric. Water Manag.* **2022**, *260*, 107296. [CrossRef]
4. Liu, C.Y.; Wang, R.; Wang, W.E.; Hu, X.T.; Wu, W.Y.; Liu, F.L. Different irrigation pressure and filter on emitter clogging in drip phosphate fertigation systems. *Water* **2022**, *14*, 853. [CrossRef]
5. Guan, Y.H.; Niu, W.Q.; Liu, L.; Li, X.K.; Zhang, W.Q. Effect of fertilizer type and concentration on sediment transport capacity of dripper in drip fertigation with muddy water. *Trans. Chin. Soc. Agric. Eng.* **2018**, *34*, 78–84, (In Chinese with English abstract). [CrossRef]
6. Khaled, E.M.; Stucki, J.W. Iron oxidation state effects on cation fixation in smectites. *Soil Sci. Soc. Am. J.* **1991**, *55*, 550–554. [CrossRef]
7. Wang, Z.Y.; Wang, W.L.; Tian, S.M. Mineral composition and distribution of the sediment in the Yellow River Basin. *J. Sediment Res.* **2007**, *5*, 3–10, (In Chinese with English abstract). [CrossRef]
8. Chen, Z.J.; Gao, J.J.; Zhao, W.Y.; Wang, C.Y.; Zhou, J.B. Effects of application of phosphorus and potassium fertilizers on ion compositions of soil solution in solar greenhouse. *Trans. CSAE* **2011**, *27*, 261–266, (In Chinese with English abstract). [CrossRef]
9. Wang, X.Y.; Wang, W.E.; Hu, X.T. Research on the emitter anti-clogging performance and system uniformity caused by fertigation. *China Rural. Water Hydropower.* **2015**, *11*, 1–5, (In Chinese with English abstract).
10. Liu, L.; Niu, W.Q.; Wu, Z.G.; Guan, Y.H.; Li, Y. Risk and inducing mechanism of acceleration emitter clogging with fertigation through drip irrigation systems. *Trans. Chin. Soc. Agric. Mach.* **2017**, *48*, 228–236, (In Chinese with English abstract). [CrossRef]
11. Tajrishy, M.A.; Hills, D.J.; Tchobanoglous, G. Pretreatment of secondary effluent for drip irrigation. *J. Irrig. Drain. Eng.* **1994**, *120*, 716–731. [CrossRef]

12. Li, J.S.; Chen, L.; Li, Y.F. Effect of chlorination on emitter clogging and system performance for drip irrigation with sewage effluent. *Trans. Chin. Soc. Agric. Eng.* **2010**, *26*, 7–13. [CrossRef]

13. Song, P.; Li, Y.K.; Li, J.S.; Pei, Y.T. Chlorination with lateral flushing controling drip irrigation emitter clogging using reclaimed water. *Trans. Chin. Soc. Agric. Eng.* **2017**, *33*, 80–86, (In Chinese with English abstract). [CrossRef]

14. Vermeiren, T. Magnetic treatment of liquids for scale and corrosion prevention. *Anti-Corros. Methods Mater.* **1958**, *5*, 215–219. [CrossRef]

15. Wang, Z.X.; Zhao, X.; Zhang, W.Q.; Niu, W.Q. Effect of magnetization of irrigation water on the clogging of drip irrigation emitters with integrated water and fertilizer. *Trans. Chin. Soc. Agric. Eng.* **2021**, *37*, 127–135, (In Chinese with English abstract). [CrossRef]

16. Rav-Acha, C.; Kummel, M.; Salamon, I.; Adin, A. The effect of chemical oxidants on effluent constituents for drip irrigation. *Water Res.* **1995**, *29*, 119–129. [CrossRef]

17. Li, Y.K.; Zhou, B.; Yang, P.L. Research advances in drip irrigation emitter clogging mechanism and controlling methods. *J. Hydraul. Eng.* **2018**, *49*, 103–114. [CrossRef]

18. Tayel, M.Y.; Pibars, S.K.; Mansour, A.G. Effect of drip irrigation method, nitrogen source, and flushing schedule on emitter clogging. *Agric. Syst.* **2013**, *4*, 131–137. [CrossRef]

19. Zhou, B.; Li, Y.K.; Liu, Y.Z.; Xu, F.P.; Pei, Y.T.; Wang, Z.H. Effect of drip irrigation frequency on emitter clogging using reclaimed water. *Irrig. Sci.* **2015**, *33*, 221–234. [CrossRef]

20. Al-Mefleh, N.K.; Talozi, S.; Naser, K.A. Assessment of treated wastewater reuse in drip irrigation under different pressure conditions. *Water* **2021**, *13*, 1033. [CrossRef]

21. Feng, D.; Kang, Y.H.; Wan, S.Q.; Liu, S.P. Lateral flushing regime for managing emitter clogging under drip irrigation with saline groundwater. *Irrig. Sci.* **2017**, *35*, 217–225. [CrossRef]

22. Liu, J.S.; Li, Y.F.; Wang, J.; Wang, Z. Microirrigation in China: History, current situation and prospects. *J. Hydraul. Eng.* **2016**, *47*, 373–381. [CrossRef]

23. Zhao, X.K.; Mo, Y.; Xia, H.; Gong, Y.T.; Wang, J.D.; Zhang, Y.Q.; Gong, S.H.; Li, Q.L. Hydraulic performance of automatic flushing valve at the end of dripline. *J. Irrig. Drain.* **2021**, *40*, 105–112. [CrossRef]

24. Mo, Y.; Zhao, X.K.; Wang, J.D.; Zhang, Y.Q.; Gong, S.H.; Xia, H.; Li, Q.L.; Wang, Y. Design and structural optimization of the automatic flushing valve with exhaust function. *Trans. Chin. Soc. Agric. Eng.* **2022**, *38*, 72–79, (In Chinese with English abstract). [CrossRef]

25. Puig-Bargues, J.; Lamm, F.R.; Trooien, T.P.; Clark, G.A. Effect of dripline flushing on subsurface drip irrigation systems. *Trans. ASABE* **2010**, *53*, 147–155. [CrossRef]

26. Han, S.Q.; Li, Y.K.; Xu, F.P.; Sun, D.X.; Feng, J.; Liu, Z.Y.; Wu, R.N.; Wang, Z.H. Effect of lateral flushing on emitter clogging under drip irrigation with Yellow River water and a suitable method. *Irrig. Drain.* **2018**, *67*, 199–209. [CrossRef]

27. Yu, L.M.; Li, N.; Liu, X.G.; Yang, Q.L.; Long, J. Influence of flushing pressure, flushing frequency and flushing time on the service life of a labyrinth-channel emitter. *Biosyst. Eng.* **2018**, *172*, 154–164. [CrossRef]

28. Zhang, W.Q.; Niu, W.Q.; Li, X.K.; Lu, M.; Yang, X.K.; Wen, S.L. Determination of first lateral flushing time and period to mitigate risk of emitter clogging in drip irrigation. *Trans. Chin. Soc. Agric. Eng.* **2019**, *35*, 70–77, (In Chinese with English abstract). [CrossRef]

29. Zhao, X.K. Research on Hydraulic Performance Test of Flushing Valve at End of Capillary and Its Application in Sandy Drip Irrigation System. Master's Thesis, Hebei Agricultural University, Baoding, China, 2016.

30. Li, W.J. Research on Hydrological Frequency of Rivers in Arid Areas Based on Normal Transformation. Master's Thesis, Shihezi University, Shihezi, China, 2022.

31. *GB/T 2411-2008/ISO 868: 2003*; Plastics and Ebonite—Determination of Indentation Hardness by Means of a Durometer (Shore Hardness), 1st ed. Standards Press of China: Beijing, China, 2008.

32. *GB/T 17187-2009/ISO 9261: 2004*; Agricultural Irrigation Equipment—Emitters and Emitting Pipe—Specification and Test Methods. Standards Press of China: Beijing, China, 2010.

33. *GB/T 19812. 2-2017*; Plastic Equipment for Water Saving Irrigation—Part 2: Pressure Compensating Emitter and Emitting Pipe. Standards Press of China: Beijing, China, 2017.

34. Bannayan, M.; Hoogenboom, G. Using pattern recognition for estimating cultivar coefficients of a crop simulation model. *Field. Crop. Res.* **2009**, *111*, 290–302. [CrossRef]

35. Dettori, M.; Cesaraccio, C.; Motroni, A.; Spano, D.; Duce, P. Using ceres-wheat to simulate durum wheat production and phenology in Southern Sardinia. *Field. Crop. Res.* **2011**, *120*, 179–188. [CrossRef]

36. Xu, Y.B.; Zhang, J.; Long, Z.Q.; Tang, H.Z.; Zhang, X.G. Hourly urban water demand forecasting using the continuous deep belief echo state network. *Water* **2019**, *11*, 351. [CrossRef]